Electronic Supplementary Material (ESI) for ChemComm.
This journal is © The Royal Society of Chemistry 2014

Electronic Supporting Information (ESI) for

Hybrid with Uniaxial Negative Thermal Expansion Behavior: Synergistic Role of Organic and Inorganic Components

Kai-Yao Wang,[a] Mei-Ling Feng,[a] Liu-Jiang Zhou,[a] Jian-Rong Li,[a] Xing-Hui Qi[a,b] and Xiao-Ying Huang*[,a]

[a] State Key Laboratory of Structural Chemistry, Fujian Institute of Research on the Structure of Matter, the Chinese Academy of Sciences, Fuzhou, Fujian 350002, P.R. China. E-mail: xyhuang@fjirsm.ac.cn; Fax: +86 591-83793727; Tel: +86-591 83793727.

[b] College of Chemistry, Fuzhou University, Fuzhou, Fujian 350002, P.R. China

1. Synthesis

Synthesis of **1**: A mixture of Sb (0.061 g, 0.5 mmol), Mn (0.027 g, 0.5 mmol), S (0.096 g, 0.5 mmol), 3.0 mL N-(3-aminopropyl)-imidazole (api) (98%) and 0.2 mL $N_2H_4 \cdot H_2O$ (99%) was sealed in a stainless steel reactor with 20 mL Teflon liner, heated at 160 °C for 8 days, and then cooled to room temperature. The product contained lamellar dark yellow crystals of **1** and black powder. The crystals of **1** were selected by hand, washed with distilled water and ethanol, and then dried in the air. The yield of the crystals of **1** is 0.083 g, 52% based on Sb. Anal. Calc. for $C_6H_{11}Mn_2N_3S_5Sb_2$ (**1**): C, 11.28%; H, 1.74%; N, 6.58%; found: C, 11.19%; H, 1.85%; N, 6.83%.

2. Crystal Structures

Single-crystal X-ray diffraction data of **1-100K**, **1-150K**, **1-200K**, **1-273K**, **1-323K**, **1-373K** and **1-473K** were collected on an SuperNova Oxford diffractometer with graphite monochromated Mo$K\alpha$ radiation (λ = 0.71073 Å) at 100 K, 150K, 200 K, 273 K, 323K, 373 K and 473 K, respectively. The absorption corrections were applied using a multi-scan technique. The structures were solved by direct methods and refined by full-matrix least-squares on F^2 using the SHELX-97 program.[1] Non-

hydrogen atoms were refined with anisotropic displacement parameters and the hydrogen atoms bonded to C and N atoms were positioned with idealized geometry. The empirical formula was confirmed by the TGA and elemental analysis. A summary of the crystal data is given in Tables S1 and S2.

Table S1 Summary of crystal data for **1-100K**, **1-150K**, **1-200K** and **1-273K**.

Compound	**1-100K**	**1-150K**	**1-200K**	**1-273K**
Empirical formula	$C_6H_{11}Mn_2N_3S_5Sb$	$C_6H_{11}Mn_2N_3S_5Sb$	$C_6H_{11}Mn_2N_3S_5Sb$	$C_6H_{11}Mn_2N_3S_5Sb$
	2	2	2	2
Formula weight	638.86	638.86	638.86	638.86
Crystal system	Orthorhombic	Orthorhombic	Orthorhombic	Orthorhombic
Space group	*Pbca*	*Pbca*	*Pbca*	*Pbca*
T/K	100(2)	150(2)	200(2)	273(2)
λ/ Å	0.71073	0.71073	0.71073	0.71073
a/ Å	12.4377(3)	12.4568(3)	12.4920(3)	12.5276(4)
b/ Å	12.2724(4)	12.2988(3)	12.3011(4)	12.3171(5)
c/ Å	21.0852(6)	21.0020(5)	20.9270(6)	20.8638(8)
α/°	90	90	90	90
β/°	90	90	90	90
γ/°	90	90	90	90
V/ Å^3	3218.45(16)	3217.58(14)	3215.75(16)	3219.4(2)
Z	8	8	8	8
D_c/ Mg·m^{-3}	2.637	2.638	2.639	2.636
μ/mm^{-1}	5.487	5.489	5.492	5.485
F(000)	2400	2400	2400	2400
Measured refls.	10373	10874	10387	10436
Independent refls.	3513	3405	3501	3512
R_{int}	0.0249	0.0290	0.0274	0.0285
No. of parameters	169	169	173	173
GOF	1.005	1.006	1.009	1.004
[a]R_1, wR_2 [$I > 2\sigma(I)$]	0.0211, 0.0496	0.0230, 0.0518	0.0248, 0.0512	0.0271, 0.0615
R_1, wR_2 (all data)	0.0251, 0.0521	0.0279, 0.0551	0.0306, 0.0545	0.0353, 0.0672

[a]$R_1 = \sum||Fo|-|Fc||/\sum|Fo|$, $wR_2 = \{\sum w[(Fo)^2 - (Fc)^2]^2/\sum w[(Fo)^2]^2\}^{1/2}$

Table S2 Summary of crystal data for **1-323K**, **1-373K**, and **1-473K**.

Compound	**1-323K**	**1-373K**	**1-473K**
Empirical formula	$C_6H_{11}Mn_2N_3S_5Sb_2$	$C_6H_{11}Mn_2N_3S_5Sb_2$	$C_6H_{11}Mn_2N_3S_5Sb_2$
Formula weight	638.86	638.86	638.86
Crystal system	orthorhombic	orthorhombic	orthorhombic
Space group	*Pbca*	*Pbca*	*Pbca*
T/K	323(2)	373(2)	473(2)
λ/ Å	0.71073	0.71073	0.71073
a/ Å	12.5694(5)	12.5883(5)	12.6068(7)
b/ Å	12.3552(5)	12.3520(5)	12.3619(8)
c/ Å	20.8407(9)	20.8164(8)	20.8422(13)
α/°	90	90	90
β/°	90	90	90
γ/°	90	90	90
V/ Å^3	3236.5(2)	3236.8(2)	3248.1(3)
Z	8	8	8
D_c/ Mg·m^{-3}	2.622	2.622	2.613
μ/mm^{-1}	5.456	5.456	5.437
F(000)	2400	2400	2400
Measured refls.	10944	10487	10428
Independent refls.	3423	3532	3546
R_{int}	0.0308	0.0305	0.0663
No. of parameters	173	173	191
GOF	1.004	1.009	1.008
[a]R_1, wR_2 [$I > 2\sigma(I)$]	0.0280, 0.0621	0.0305, 0.0667	0.0441, 0.1000
R_1, wR_2 (all data)	0.0373, 0.0689	0.0425, 0.0755	0.0639, 0.1184

[a]$R_1 = \sum||Fo|-|Fc||/\sum|Fo|$, $wR_2 = \{\sum w[(Fo)^2 - (Fc)^2]^2/\sum w[(Fo)^2]^2\}^{1/2}$

Table S3. Summary of a, b, c, L_1, L_2, L_3, δ, ε for **1** in different temperatures.

T (K)	a (Å)	b (Å)	c (Å)	L_1 (Å)	L_2 (Å)	L_3 (Å)	δ (°)	ε (°)
100	12.4377(3)	12.2724(4)	21.0852(6)	12.2724(7)	10.9660(6)	4.9919(35)	68.052(4)	30.831(3)
150	12.4568(3)	12.2988(3)	21.0020(5)	12.2988(8)	10.9404(7)	4.9763(39)	68.400(4)	31.110(3)
200	12.4920(3)	12.3011(4)	20.9270(6)	12.3011(8)	10.9066(8)	4.9374(45)	68.656(5)	31.432(4)
273	12.5276(4)	12.3171(5)	20.8638(8)	12.3171(10)	10.8732(9)	4.8906(53)	68.999(6)	31.797(4)
323	12.5694(5)	12.3552(5)	20.8407(9)	12.3552(10)	10.8693(9)	4.8618(55)	69.271(6)	32.033(4)
373	12.5883(5)	12.3520(5)	20.8164(8)	12.352(1)	10.8533(9)	4.8455(61)	69.367(6)	32.233(4)
473	12.6068(7)	12.3619(8)	20.8422(13)	12.3619(16)	10.8433(15)	4.8096(88)	69.504(10)	32.444(7)

Table S4 The changes of $d_{thickness}$ in the temperature range of 100-473K.[a]

T (K)	φ1 (°)	φ2 (°)	d(Mn2⋯Mn1) (Å)	d(Mn2'-Mn1) (Å)	d(Mn2⋯Mn1) *cos(φ1) (Å)	d(Mn2'⋯Mn1) *sin(φ2-90°) (Å)	Sum (Å)
100K	66.437	102.691	3.8481	5.4632	1.5383	1.2002	2.7385
150K	66.427	102.752	3.8611	5.4799	1.5441	1.2096	2.7573
200K	66.336	102.884	3.869	5.4964	1.5529	1.2256	2.7785
273K	66.245	103.096	3.8848	5.5197	1.5649	1.2507	2.8156
323K	66.247	103.209	3.9027	5.5448	1.572	1.267	2.839
373K	66.223	103.354	3.9073	5.5572	1.5753	1.2835	2.8588
473K	66.118	103.625	3.9213	5.5819	1.5876	1.3149	2.9025

[a] The $d_{thickness}$ is calculated by the following formula: $d_{thickness}$ = d(Mn2⋯Mn1)*cos(φ1) + d(Mn2'⋯Mn1)*sin(φ2-90°). All the distances and angles are measured by Diamond v3.2 software. (see Figure S2)

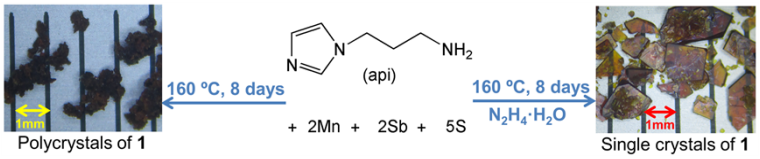

Scheme 1. Reaction pathway for the formation of $Mn_2(api)Sb_2S_5$ (**1**).

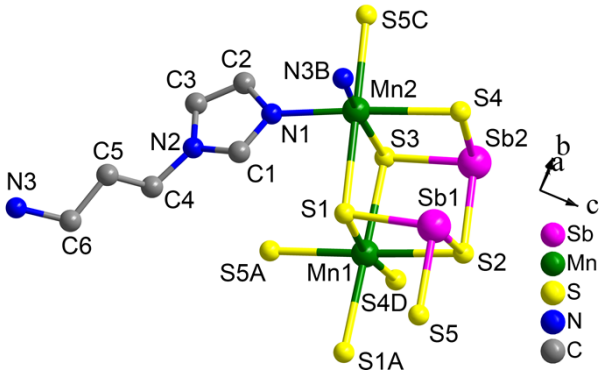

Fig. S1 Crystallographically asymmetric unit in **1-100K** and the coordination geometries of metal ions. Symmetry codes for generated atoms: A) 1-*x*, 1-*y*, 1-*z*; B) 1-*x*, 0.5+*y*, 0.5-*z*; C) 0.5+*x*, 1.5-*y*, 1-*z*; D) 1.5-*x*, -0.5+*y*, *z*.

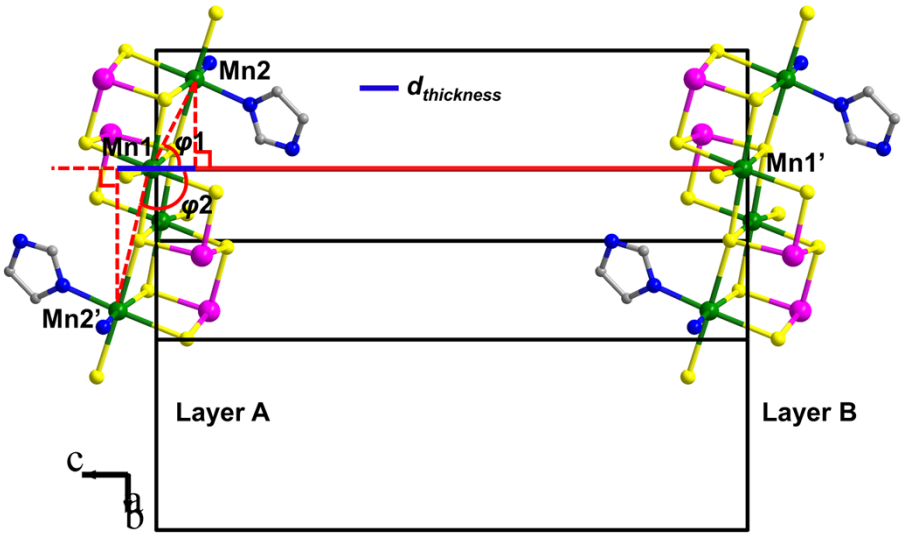

Fig. S2 The representation of the single-layer thickness ($d_{thickness}$) by using the vertical distance between two Mn2 atoms in one $\{Mn_2Sb_2S_5\}_n$ layer.

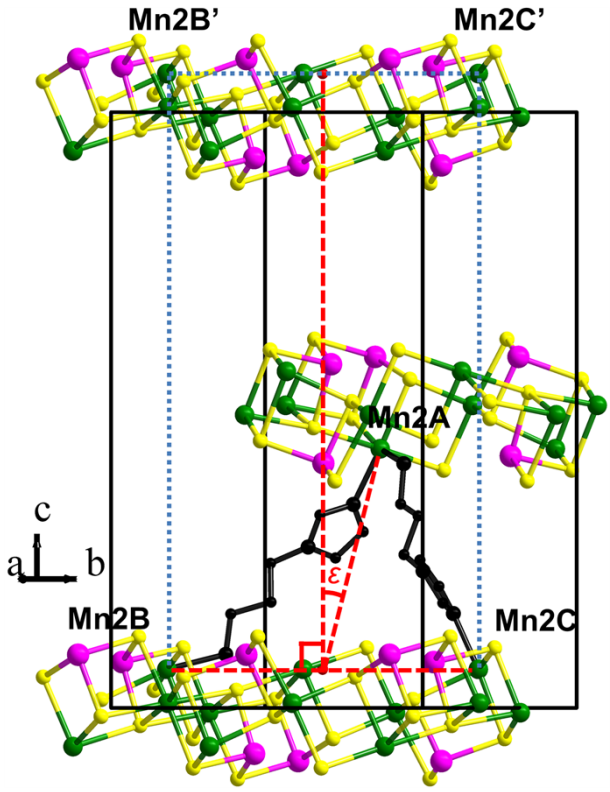

Fig. S3 The representation of angle (ε) between plane going through Mn2A, Mn2B, Mn2C and the normal to the $\{Mn_2Sb_2S_5\}_n$ plane. The extra red balls represent the middle point of Mn2B···Mn2C.

3. Materials and physical measurements

All reagents and chemicals were purchased from commercial sources and were used without further purification. Elemental analyses for C, H and N were performed on a German Elementary Vario EL III instrument. Energy dispersive spectroscopy (EDS) was obtained with a JEOL JSM-6700F scanning electron microscope. The UV/Vis spectrum was measured at room temperature using a PE Lambda 950 UV/Vis spectrophotometer, and a $BaSO_4$ plate was used as a standard (100% reflectance). The absorption spectrum was calculated from reflectance spectrum by using the function: $\alpha/S = (1-R^2)/2R$, [2] where α is the absorption coefficient, S is the scattering coefficient, and R is the reflectance. Variable-temperature powder X-ray diffraction (PXRD) patterns for **1** were collected in the angular range of 2θ = 3-52° on a Rigaku DMX/2000 diffractometer using Cu$K\alpha$ radiation. PXRD on the TGA residue of **1** was collected in the angular range of 2θ = 3-65° on a Miniflex II diffractometer using Cu$K\alpha$ radiation. A NETZSCH STA 449C thermogravimetric analyzer was used to obtain thermogravimetric (TG) curves in a N_2 atmosphere with a heating rate of 5 °C /min in the temperature range of 20-500 °C.

3a) EDS

Data collected from five points on the surface of one single crystal of **1** confirmed that the average Mn: Sb: S ratio was 1: 1.14: 2.58, close to the ideal ratio of 1: 1: 2.5.

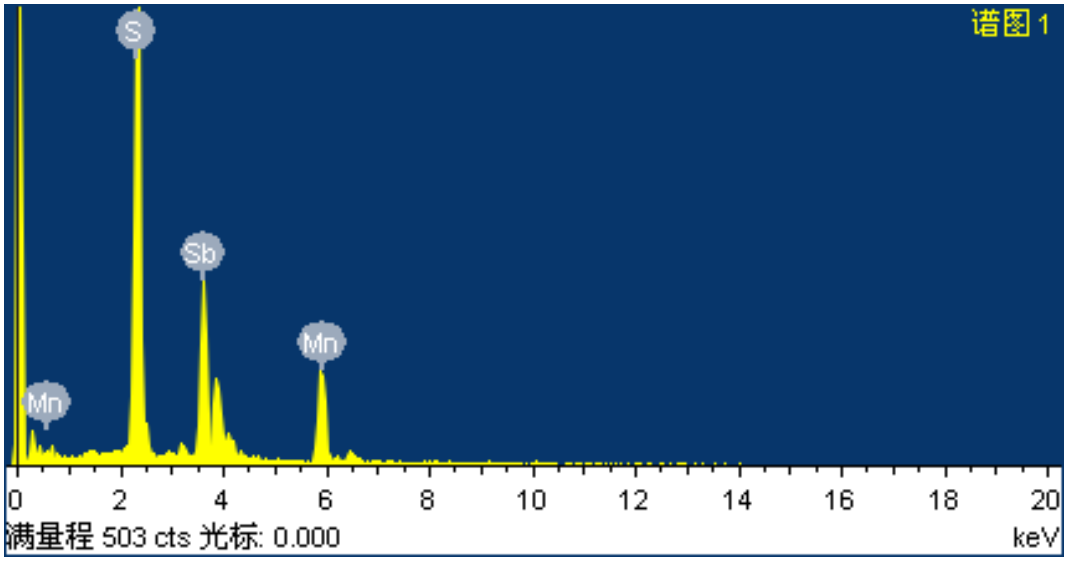

Fig. S4 The energy dispersive spectroscopy (EDS) of **1**.

3b) TGA and PXRD of the TG residue

The TG curve of compound **1** (Figure S5a) displays one main step weight loss of 19.9% (theoretical value of 19.5%) from 305 to 360 ºC, corresponding to the loss of one api ligand in the formula of **1**. From the Figure S5b, it indicates that the residue of **1** after TGA is a mixture of $MnSb_2S_4$ and MnS.

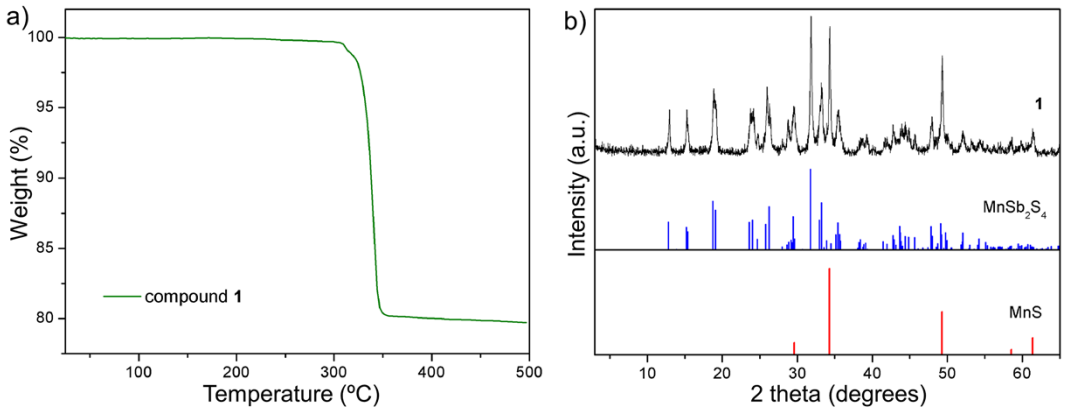

Fig. S5 (a) Thermogravimetric curve for **1**. (b) The PXRD pattern of the TG residues of **1**.

3c) PXRD of the single crystal and poly crystal of 1

The identical PXRD patterns shown in Figure S6 illustrate the same product

obtained from the reaction mixture with or without the addition of $N_2H_4 \cdot H_2O$. The key point of adding $N_2H_4 \cdot H_2O$ is to enhance the quality and dimension of the crystals.

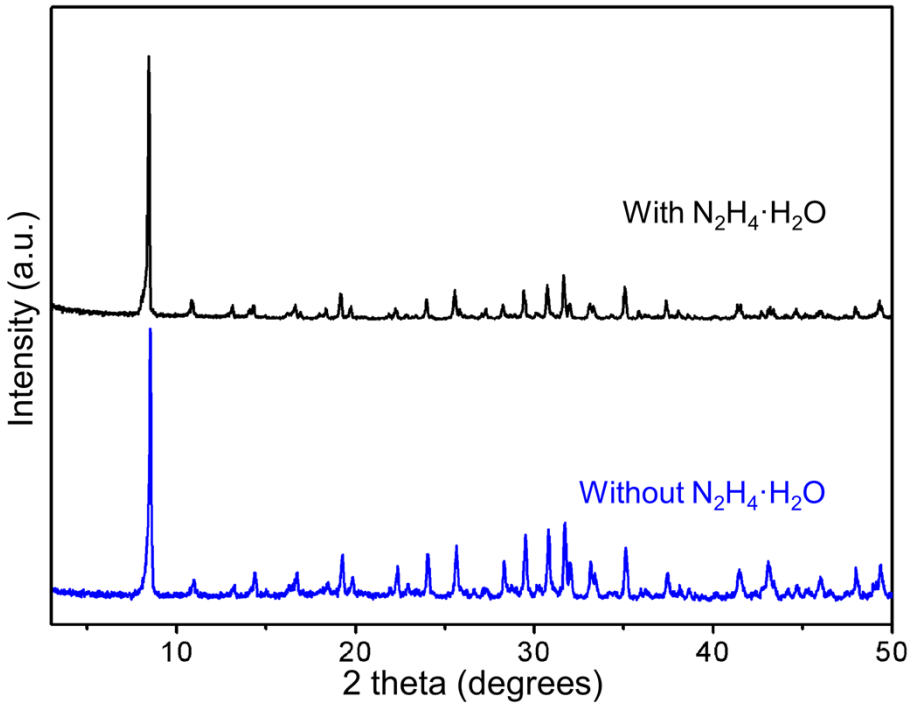

Fig. S6 PXRD patterns for the products from the preparative reactions of **1** with (black curve) or without (blue curve) adding $N_2H_4 \cdot H_2O$ in the reaction mixture.

3d) Variable-temperature powder X-ray diffraction (PXRD) patterns and lattice parameters obtained from least-squares refinement

The powder X-ray diffraction (PXRD) patterns were recorded over the temperature range 100-473K, Figure S7. When temperature increases, the 2θ values of (002) and (006) peaks shift from 8.32 and 25.28 ° at 100 K to 8.50 and 25.60 ° at 473 K, respectively, directly reflecting the gradual decrease of c parameter. In contrast, the position of (020) peak shows a decreasing tendency from 14.37 ° at 100 K to 14.28 ° at 473 K, in consist with enlargement of b parameter. Lattice parameters obtained from least-squares refinement demonstrate the NTE with the average α (100-373K) of thermal expansion of -47×10^{-6} K^{-1}, in a good agreement with that documented by SC-XRD, Figure S8.

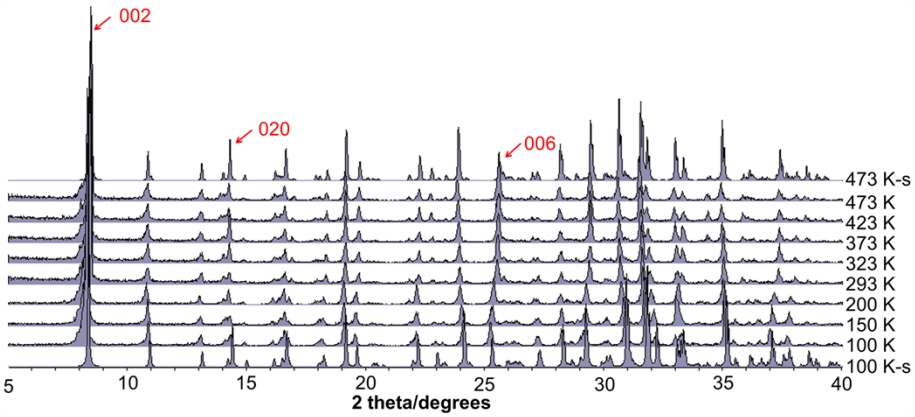

Fig. S7 (a) Temperature-dependent PXRD patterns of **1**. Top and bottom are simulated patterns of **1-473K** and **1-100K**.

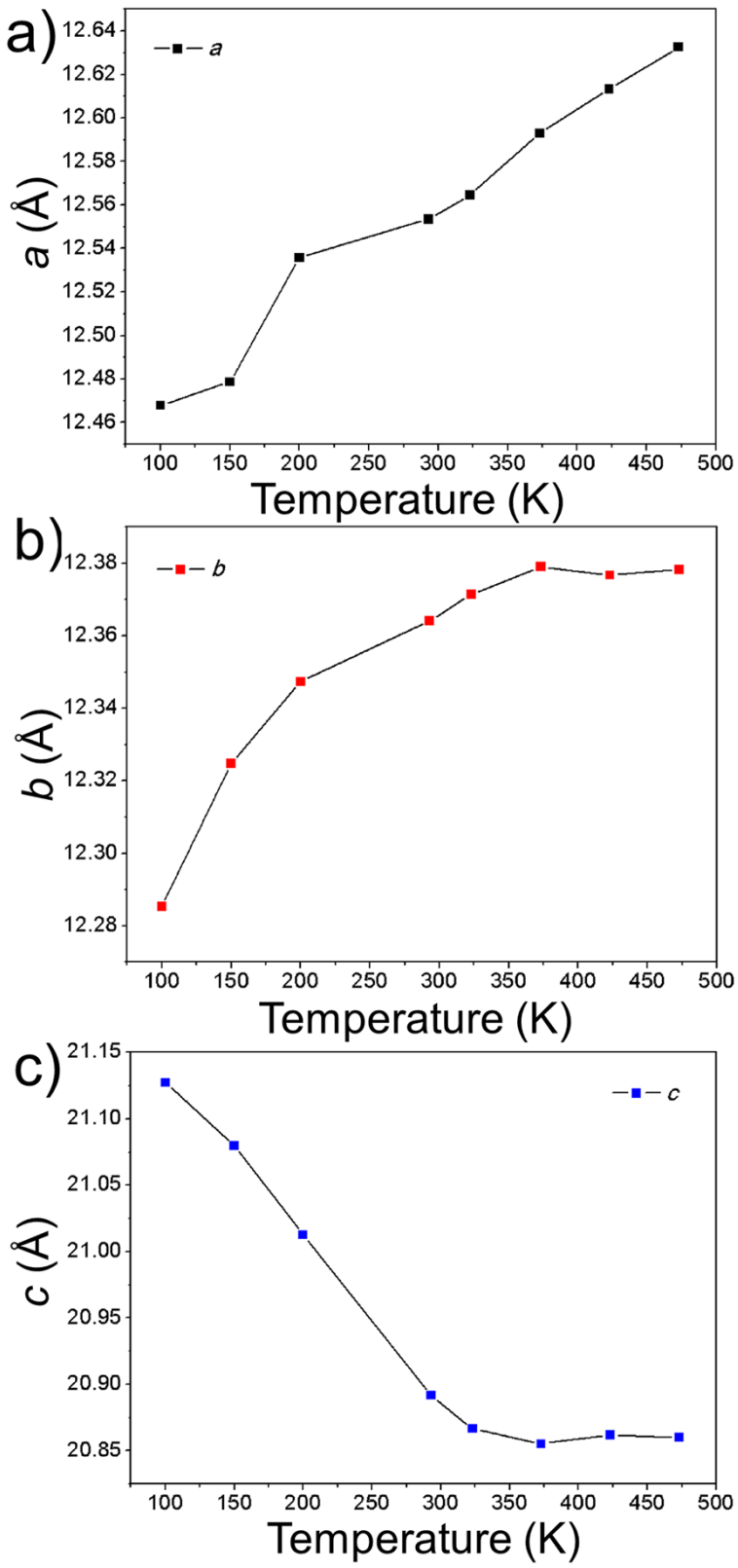

Fig. S8 Changes of lattice parameters of (a) *a*, (b) *b* and (c) *c* axes obtained from least-squares refinements of the PXRD data by using Jade 5.0 software.

3e) Solid-state UV-Vis absorption spectrum

Solid-state UV-Vis absorption spectrum reveals the optical band gap (E_g) of **1** is 2.38 eV, Figure S9. This value is comparable to that of $[Mn_2(phen)(Sb_2S_5)]_n$ (E_g = 2.23 eV),[6] while is a bit higher than those of $[Mn_2Sb_2S_5(N_2H_4)_3]$ (E_g = 2.09 eV) [7] and $[Mn_2Sb_4S_8(N_2H_4)_2]$ (E_g = 1.59 eV).[8]

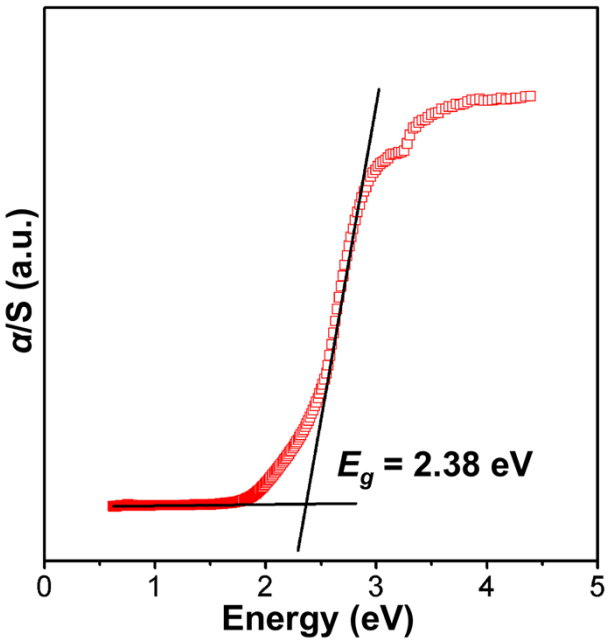

Fig. S9 Solid state absorption spectrum of compound **1**.

4. Theoretical Calculations

The DFT calculations were performed via the Vienna ab initio simulation program (VASP).[3] The Perdew-Burke-Ernzerhof (PBE) [4] functional of the generalized gradient approximations (GGA) [5] was employed as the exchange-correlation function. The valence atomic configurations were $1s^2$, $2s^22p^2$, $2s^22p^3$, $3s^23p^4$, $3d^54s^2$ and $4d^{10}5s^25p^3$ for H, C, N, S, Mn and Sb, respectively. The plane-wave cutoff energy of 400 eV and the threshold of 10^{-5} eV were set for the self-consistent-field convergence of the total electronic energy. For density of states (DOS) calculations, we used a 5×5×3 Monkhorst-Pack k-point grid within the Brillouin zone. Because of the correlation effect of Mn 3d states, the GGA + U method with U = 4 eV were employed. A large U = 6 eV was also tested, but the band gap is similar to U = 4 eV.

DFT calculations on the band structures indicate compound **1** is an indirect semiconductor with a band gap of 2.36 eV, close to the experimental value, Figure

S10. The calculations on DOS reveal that the conduction band minimum above the Fermi level is mainly contributed by Sb-5p and S-3p states, while the top of valence band is dominated by Mn-3d and S-3p states, Figure S11.

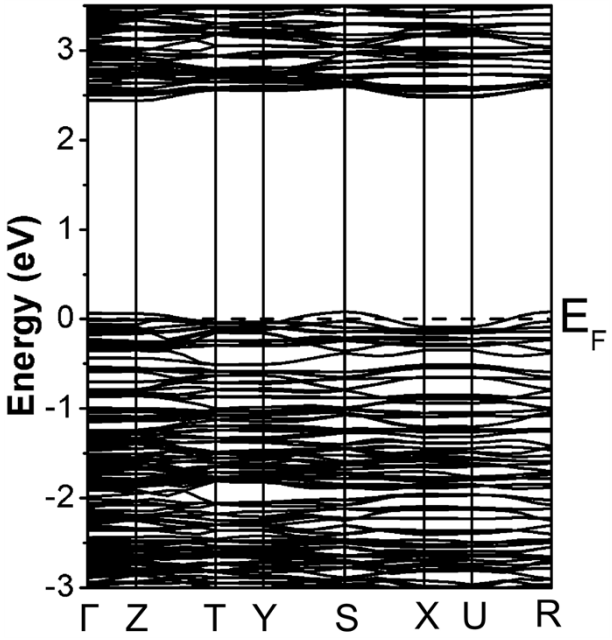

Fig. S10 The band structures of **1**. Fermi level is set at 0 eV (dashed line).

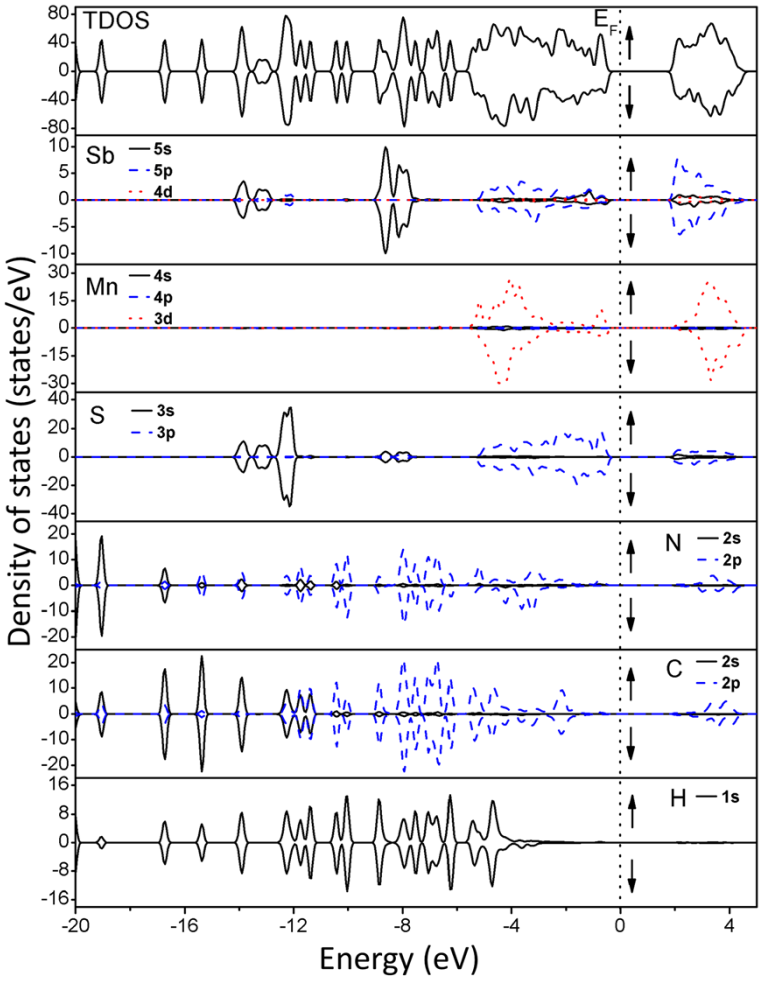

Fig. S11 The total density of states and partial density of states for **1**. The Fermi level is set at 0 eV (dotted line).

5. Magenetic Property Study

The magnetic behavior of **1** was studied by measuring the direct current (dc) temperature-dependent magnetic susceptibility (2-300k) on the pure crystalline sample with a Quantum Design PPMS 6000 magnetometer under an applied field of 1000 Oe, Figure S12. The $\chi_M T$ product a 6.62 emu K mol^{-1} at 300 K, and continuously decrease to 0.24 emu K mol^{-1} upon cooling to 2 K, suggesting an antiferromagnetic behavior. The inverse magnetic susceptibility χ_M^{-1} in the temperature range of 75-100 K can be fitted well to the Curie-Weiss equation $\chi_M^{-1} = (T - \theta)/C$ with the Curie constant C = 8.86 emu K mol^{-1} and the Weiss constant θ = -101.8 K, confirming a strong antiferromagnetic exchange interaction.[9] The effective magnetic moment (μ_{eff}) for one Mn^{2+} in the compound **1** is 4.21 μ_B, which is in agreement with high spin Mn^{2+} configuration known from MnS and MnS_2.[10]

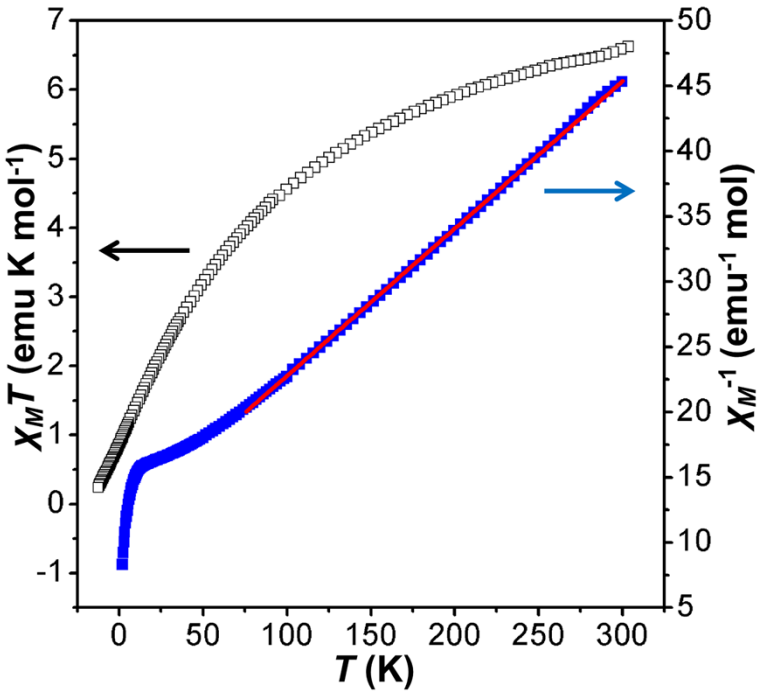

Fig. S12 The plots $\chi_M T$ and χ_M^{-1} vs. T for **1**.

References

1. G. M. Sheldrick, *SHELXS97 and SHELXL97*, University of Göttingen, Germany, **1997**.
2. W. M. Wendlandt, H. G. Hecht, *Reflectance Spectroscopy*, Interscience, New York, **1966**.
3. G. Kresse, D. Joubert, *Phys. Rev. B*, **1999**, *59*, 1758-1775.
4. J. P. Perdew, K. Burke, M. Ernzerhof, *Phys. Rev. Lett.*, **1996**, *77*, 3865-3868.
5. G. Kresse, J. Furthmüller, *Phys. Rev. B*, **1996**, *54*, 11169-11186.
6. X. Wang, T.-L. Sheng, S.-M. Hu, R.-B. Fu, X.-T. Wu, *Inorg. Chem. Commun.*, **2009**, *12*, 399-401.
7. Y. Liu, P. D. Kanhere, C. L. Wong, Y. Tian, Y. Feng, F. Boey, T. Wu, H. Chen, T. J. White, Z. Chen, Q. Zhang, *J. Solid State Chem.*, **2010**, *183*, 2644-2649.
8. Y. Liu, Y. Tian, F. Wei, M. S. C. Ping, C. Huang, F. Boey, C. Kloc, L. Chen, T. Wu, Q. Zhang, *Inorg. Chem. Commun.*, **2011**, *14*, 884-888.
9. L. Engelke, R. Stähler, M. Schur, C. Näther, W. Bensch, R. Pöttgen, M. H. Möller, *Z. Naturforsch.,* **2004**, *59b*, 869-876;
10. (a) Y. Liu, Y. Tian, F. Wei, M. S. C. Ping, C. Huang, F. Boey, C. Kloc, L. Chen, T. Wu, Q. Zhang, *Inorg. Chem. Commun.*, **2011**, *14*, 884-888; (b) S. F. Matar, R. Weihrich, D. Kurowski, A. Pfitzner, V. Eyert, *Phys. Rev. B*, **2005**, *71*, 235207.